# Environmental Science
## Processes & Impacts

Accepted Manuscript






ROYAL SOCIETY OF CHEMISTRY

rsc.li/process-impacts

The data shown in this work demonstrate that viable *S. putrefaciens* (and most likely some other microorganisms) has a great potential to stabilise (or reduce the mobility in the environment of) $Mn^{2+}$ (and most likely some other metal ions) through processes occurring at the interfaces of the cells for at least 30 days. The interfacial processes start from ion exchange/surface complexation and continue with biomineralisation. Composition of bioprecipitates is a function of temperature, metal loading and bacterial density. The results presented demonstrate that the role of microorganisms in formation of natural minerals might be even greater than thought preciously.

# Formation of manganese phosphate and manganese carbonate during long-term sorption of $Mn^{2+}$ by viable *Shewanella putrefaciens*: effects of contact time and temperature

**Natalia Chubar[1,2*], Cristina Avramut[1] and Tom Visser[3]**

[1]Utrecht University, Department of Earth Sciences, Budapestlaan 4, 3584 CD, Utrecht, The Netherlands

[2]School of Engineering and Built Environment, Glasgow Caledonian University, Cowcaddens Road 70, G4 0BA, Glasgow, United Kingdom

[3] Utrecht University, Department of Inorganic Chemistry and Catalysis, Sorbonnelaan 16, 3584 CA, Utrecht, The Netherlands

**Key words** *Shewanella putrefaciens*, $Mn^{2+}$, biosorption, biomineralisation, temperature, Mn phosphate, Mn carbonate, extracellular polymeric substances, FTIR, EXAFS

* Corresponding author (present address): N. Chubar, School of Engineering and Built Environment, Glasgow Caledonian University, Cowcaddens Road 70, Glasgow, G4 0BA, United Kingdom; e-mail: Natalia.Chubar@gcu.ac.uk; Phone: +44-141-2731779.

ABSTRACT

The influence of temperature (5, 10, 22 and 30 °C) on the long-term (30 days) sorption of $Mn^{2+}$ by viable *Shewanella putrefaciens* was studied by FTIR and EXAFS. The additional Mn-removal capacity of these bacteria was found to result from the surface precipitation of Mn-containing inorganic phases. The chemical composition of the Mn-containing precipitates is temperature and contact-time dependent. Mn (II) phosphate and Mn (II) carbonate were the two major precipitates formed in 1000-ml batches at 10, 22 and 30 °C. The ratio of Mn (II) phosphate to Mn (II) carbonate was a function of the contact time. After 30 days, $MnCO_3$ was the dominant phase in the precipitates at 10, 22 and 30 °C; however, $MnCO_3$ did not form at 5 °C. Mn (II) phosphate was the only precipitate formed at 5 °C over 30 days. The biosynthesis of Extracellular Polymeric Substances (EPS) was much greater at the lowest temperature (5 °C); however, these polymeric sugars did not contribute to the additional removal of Mn(II) under the experimental conditions. This work is one of the first reports demonstrating the ability of microbes to bioprecipitate manganese phosphate and manganese carbonate. Because of the focus on interfacial processes, this is the first report showing a molecular-level mechanism for manganese carbonate formation (in contrast to the traditionally studied aged minerals).

## Introduction

Microorganisms are well known to play a key role in the cycling of chemical elements in the environment on a global scale, but many molecular-level processes that control such transformations are poorly understood. In 1986, the leading role of bacteria in iron-silica crystalline nucleation was discovered,[1] and the hypothesis that bacteria can be the nucleation sites for authigenic minerals was proposed one year later[2] which was confirmed by the same authors.[3] Since that time, studies of the roles of microbes in the formation and dissolution of various minerals have resulted in much new knowledge in geochemistry and geology. Manganese attracts special attention from geoscientists because this chemical element forms a variety of precipitates in natural ecosystems, and these precipitates control the cycling of nutrients and xenobiotics in the environment through adsorption, dissolution, and redox transformation processes.[4-6] Various hydrous oxides of manganese (III, IV) and manganese carbonate ($MnCO_3$) are usually discussed. Less attention has been given to manganese phosphates. Biogenic manganese oxides are highly abundant in the environment.[7-8] They are reactive and control many redox reactions with organic and inorganic substances. A number of studies have demonstrated that biological Mn(II) oxidation dominates in the environment.[9-10] Mn-oxides produced by the Mn-oxidising bacteria *Leptotricht discophora*[11-12] and *Bacillus sp.*[13-14] have been studied extensively. Interesting research has been conducted to isolate new, diverse Mn(II)-oxidising bacteria from deep environments.[15]

Manganese carbonate occurs naturally as the mineral rhodochrosite.[4] Rhodochrosite is rarely in its pure form and primarily forms solid solutions with carbonates of iron, calcium, zinc. Recently, the role of microorganisms in the formation of $MnCO_3$ was studied using samples of Mn-carbonate ores collected at Adilabad, India,[16] and Sichuan Province, China.[17] Mukhopadhyay[16] concluded that the formation process of Mn-carbonate was induced by microbes and continued through abiotic precipitation and growth of the previously formed crystals. Fan[17] found that Gayan Mn-carbonate ores

were rich in organic matter and that microbially inducted sulphate reduction played an important role in the formation of these ores during early diagenesis. Manganese phosphates are currently known to be less widely distributed in the environment than manganese carbonates. Manganese phosphates are often solid solutions rich in lithium and iron, $Li(Mn, Fe)PO_4$, and with other metals (such as Mg, Ca, Al, Zn, K, Cu and others). A manganese phosphate mineral was characterised by Kampf[18]; however, new manganese phosphate species have been discovered by Fransolet[19] and recently by Cooper[20] what is most likely not the last discovery of new phosphate minerals. Laboratory studies of biogenic precipitation usually address the molecular-level process of the oxidation of redox metals by oxidising microbes (biogenic metal oxides) or use aged minerals (carbonate formation). The role of microorganisms in the formation of manganese carbonates in different regions of the globe has been demonstrated.[17,21-23] However, only aged manganese carbonate minerals were studied, so (indirect) theoretical conclusions were found instead of experimental evidence. Molecular level research, which would demonstrate the formation process of $MnCO_3$, has not been conducted to date.

For manganese phosphates, the initial study, which showed that microbes also played an important role in the formation of manganese phosphate minerals, was the recent work by the authors.[24] This study resulted from the non-traditional decision to study the sorption of manganese, a redox metal in the reduced state, $Mn^{2+}$, by the reducing bacteria, viable *Shewanella putrefaciens*. The authors discovered the capacity of viable *S. putrefaciens* to sorb $Mn^{2+}$ over 30 days despite the previously unknown ability of these microbes to form Mn-phosphates. To deepen knowledge about the novel processes at the interface of viable cells of *Shewanella putrefaciens* with aqueous $Mn^{2+}$, additional experiments were performed to define the influence of various temperatures (5, 10, 22 and 30 °C) on Mn(II) sorption, on the chemical composition of the Mn-containing precipitates formed and on the formation of EPS. These experiments resulted in a new discovery. Changing the experimental conditions (size of the experimental batches: 125 ml in the previous work and 1000 ml in the latest) allowed discovery of the process of manganese carbonate formation. This formation took place a few

days after the experiments started and at a later stage than the formation of manganese phosphates. (Manganese carbonates were not formed in 125 ml batches.) These results, which differ from those in the previous work,[24] are shown in the current work. This paper is the first report showing the molecular level processes of manganese carbonate formation initiated by microbes (in contrast to the previously studied aged minerals); this is also the first work demonstrating how the bioprecipitation process of manganese phosphate can be replaced by the formation of manganese carbonate and is thus the first ever possible explanation of why manganese carbonates are much more widely spread in the environment than manganese phosphates. The role of the temperature on the rate of such processes and the chemical composition of the precipitates has also been demonstrated.

The main tasks of this work were to study the temperature (5, 10, 22 and 30 $^{o}$C) influence on $Mn^{2+}$ sorption by viable *Shewanella putrefaciens* over one month and to characterise precipitates formed at the interface by EXAFS and FTIR.

## Materials and Methods

### Preparation of bacterial suspensions for experiments

The classical microbiological method was followed to prepare suspensions of the viable *S. putrefaciens* strain 200R for the experiments. First, single colonies were transferred from agar plates of Luria-Bertani (LB) media to liquid LB media (5 g of yeast extract, 10 g of tryptone and 10 g of NaCl in 1 litre); then, they were cultured aerobically at room temperature (22±2°C) under continuous shaking for 24 hours. The cells (grown in the liquid LB media) were used to inoculate larger bottles of LB medium and were grown for 48 hours. This time was chosen because of the discovery of Haas,[25] who showed that surface of *S. putrefaciens* cells is most enriched in functional groups at 48 hours of growth. The cells were harvested and then were pelletised by centrifugation. They were washed five times with 0.1 M NaCl to ensure full removal of LB solution from the cells. The large volumes (500 ml) of pelletised

cells (to avoid great loss (in %) from filtration) were used to establish direct correlation between the optical density of the pelletised cells and the dry weight of the bacteria. The suspension was carefully mixed and the optical density (at the wavelength of 660 nm) was promptly recorded. The measurements were repeated five times. A 500 ml sample of the suspension (with a known optical density) was filtered through membrane filters with a pore diameter of 0.2 μm (Advanced Microdevices Pvt. Ltd.). The filtered sample was dried at room temperature, and then in an oven at 120 °C. The weight of the dried filter was preliminary measured. This procedure establishes the direct correlation between the optical density of the viable cells and the dry weight of the same cells' biomass (to be used as a unit of measurements of an adsorptive performance). This ratio remains constant in spite of the changes in the cells' viability during the long-term contact of viable cells with aqueous $Mn^{2+}$. The experiments were repeated 5 times. The values measured each time differed from the average value by no more than 10%. The average value of the ratio between the optical density and the dry weight of the microbial cells was used for future experiments. The cells' viability was changing naturally during the experiments from fully viable to (partly) inactivated what allowed involvement of both viable (1), viable but non-reproducible (2) and inactivated/dead (3) cells in the experimental system. Such experimental conditions allowed closer the laboratory experimental conditions to the conditions in real environment where all three (known) states of microbes (viable, non-reproducible and dead) coexist. In the same time the unit of measurement of adsorption science (mg of dry weight per litre) was maintained.

**Sorption experiments**

The batch adsorption investigations were performed with 1000 ml of the bacterial suspension with a density (or adsorbent dose) of 2 $g_{dw}$ $L^{-1}$. It is the traditional adsorbent dose over the last decades as often within its range between 1 and 5 $g_{dw}$ $L^{-1}$, the adsorptive performance (measured in mg $g_{dw}^{-1}$) is the same. The $Mn^{2+}$ concentration was 200 mg $L^{-1}$. Bacterial suspensions in 0.1 M NaCl were first brought

to the necessary temperature (5, 10, 22, and 30 °C). A pre-set amount of $Mn^{2+}$ (as $MnCl_2 \cdot 6H_2O$) was added to bring the concentration of the cells to 2 $g_{dw}$ $L^{-1}$ and to pre-set the concentration of $Mn^{2+}$. No nutrients except for the background electrolyte, 0.1 M NaCl added initially, were provided to the microbes during the sorption experiments. The exact concentration of the bacterial cells was analysed before and after the addition of $Mn^{2+}$. The large glass beakers containing the microbial suspension were covered with caps to protect the microbial culture from contamination. The caps were removed (opened) once a day for a few minutes to take small samples for analysis. The kinetics of Mn(II) uptake were regularly studied, but the "adsorbent" samples for the spectroscopic analyses were taken at the end of the experiments (at 30 days). We avoided frequent sampling (on a daily basis) of the "adsorbent" from the experimental batches to maintain the same experimental conditions as the kinetics studies. A few additional ambient temperature experiments were performed to collect samples after less than 30 days (in 6, 9 and 10 days) at an initial concentration of $Mn^{2+}$ of 200 mg $L^{-1}$. The samples were centrifuged, were filtered with a 0.2-μm pore diameter filter (Advance Microdevices P. LTD) and were carefully dried at ambient temperature for the spectroscopic investigations.

**Fourier Transform Infrared (FTIR) spectroscopy**

The FTIR spectra of the air-dried samples of bacteria were recorded in KBr pellets at ambient conditions with a Perkin-Elmer 2000 FTIR spectrometer equipped with a DTGS detector.[24] The sample compartment was flushed with dry air to reduce interference from $H_2O$ and $CO_2$. The optical resolution of the spectra was 4 $cm^{-1}$, and 25 scans were accumulated for each spectrum.

**EXAFS (Extended X-ray Absorption Fine Structure) and XANES (X-ray Absorption Near Edge Structure)**

The experimental and reference samples were ground to very fine powders and were mixed with boron nitride, while considering the percentage of Mn in each sample measured from the adsorption

experiments. The samples were mounted in 1-mm-thick sample holders for EXAFS and XANES data collection. The spectra were recorded at the Mn *K*-edge (6539 eV) in transmission mode at ambient temperature at the Dutch-Belgian beamline (DUBBLE) (BM 26A) of the European Synchrotron Radiation Facilities.[26] The monochromator was calibrated by assigning an energy value of 6539 eV to the first inflection point in the absorption edge of a reference foil of Mn. The data were first calibrated to 6539 eV of Eo. Both the treated and raw data were used for the data analysis. IFFEFIT program components (ATHENA, ARTHEMIS, stand-alone ATOMS from the DEMETER) were used to analyse the data through linear combination fitting and principle component analysis.[27] Ten (commercially available, see: Chubar[24]) reference substances ($Mn_3(PO_4)_2$, $MnCO_3$, $MnCl_2$, $MnSO_4$, MnO, $MnO_2$ (powder), $MnO_2$ (pyrolisite), MnO(OH) (manganite), $Mn_2O_3$, and $Mn_3O_4$) were recorded at DUBBLE and were used for analysis with the IFFEFIT programs.

**Analytical chemistry methods**

Concentrations of $Mn^{2+}$ was analysed with ICP-OES (inductively coupled plasma optical emission spectrometry). For ICP-OES, SPECTRO CIROS$^{CCD}$ (by SPECTRO Analytical Instruments GmbH – Germany) was applied through the Watertaak2004 method.

## Results

**Kinetics of Mn(II) sorption at various temperatures**

Fig. 1 shows the kinetics of the $Mn^{2+}$ sorption by viable (also referred to here as live) *S. putrefaciens* over 3 minutes (Fig. 1A), 3 hours (Fig. 1C) and 30 days (Fig. 1E). In Fig. 1E, the values begin at 1 day (no data are shown for a few seconds to a few minutes of contact time). Fig. 1 also shows the drift of the pH in the same experimental suspensions over 3 minutes (Fig. 1B), 3 hours (Fig. 1D) and 30 days (Fig. 1F).

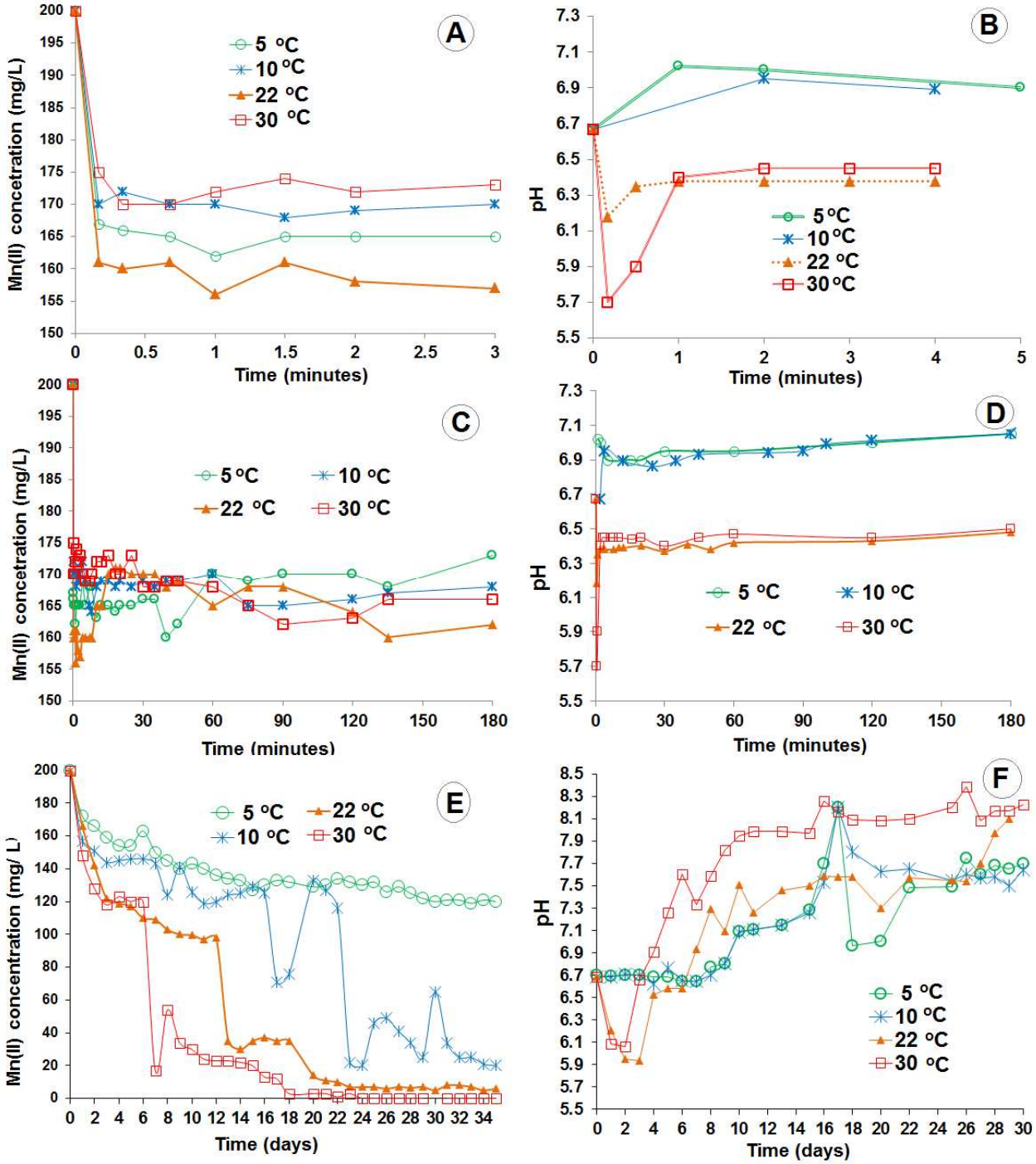


**Fig. 1** Kinetics of $Mn^{2+}$ sorption by viable *S. putrefaciens* at 5, 10, 22 and 30 °C over 3 minutes (A), 3 hours (C) and 30 days (E) and the corresponding pH drift (B, D and F). Experimental conditions: bacteria density=2 $g_{dw}$ $L^{-1}$, volume of viable bacterial suspensions=1000 ml, and initial $Mn^{2+}$ concentration=200 mg $L^{-1}$.

There was no distinct temperature (5, 10, 22 and 30 °C) influence on the $Mn^{2+}$ sorption over 3 hours contact time (Fig. 1C); however, temperature influence was observed over 30 days (Fig. 1E). The rate of Mn(II) removal increased proportionally to temperature. The periods of sharp, fast decreases of $Mn^{2+}$ in the solutions took place on days 7, 12 and 23 at 30, 22 and 10 °C, respectively; however, those periods were never observed at 5 °C over 30 days. The removal of Mn(II) at 5 °C was slow and continuous. Despite the absence of a temperature effect on Mn(II) removal over 3 hours, the pH drift in the experimental suspensions (Figs. 1B and D) demonstrated that the interfacial processes occurring at higher (22 and 30 °C) and lower (5 and 10 °C) temperatures differed from one another. In the first few minutes, when the living cells came into contact with the metal ions, the pH dropped (from 6.7 to 6.1 and to 5.7) at 22 and 30 °C but increased at 5 and 10 °C (from 6.7 to 7.0 and to 6.9). Decrease in pH at 22 and 30 $^{o}$C resulted from cation exchange of the surface $H^{+}$ for the aqueous $Mn^{2+}$ in accordance with the reaction (using an example of carboxylic functional groups):

$$\text{surface-COOH} + Mn^{2+}_{aq.} \rightarrow \text{surface-}(COO)_2Mn + 2H^{+}_{aq.}$$

The physiological pH of these microbes (i.e. the pH microbial cells maintain in 0.1 M NaCl with no $Mn^{2+}$ or other metal cations like $Cu^{2+}$ or $Zn^{2+}$ until they are viable >90%) was the same (6.7) at 5, 10, 22 and 30 °C during one week that is an observation from the blank experiments.

At 5 and 10 °C, the viable cells of *S. putrefaciens* re-established the physiological pH (6.7) in 1 day and maintained pH stability over the next 7 days while continuing to slowly sorb $Mn^{2+}$. At 22 °C, the physiological pH was re-established in 4 days, but the living cells were only able to maintain the pH for 3 days (from days 4 to 6, Fig. 1F); then, the pH increased. At 30 °C, the pH changed on a daily basis (Fig. 1F).

**FTIR spectra of S. putrefaciens exposed to aqueous $Mn^{2+}$**

Fig. 2 shows the FTIR spectra of *S. putrefaciens* exposed to 200 mg $L^{-1}$ of $Mn^{2+}$ for 30 days at 5, 10, 22 and 30 °C.

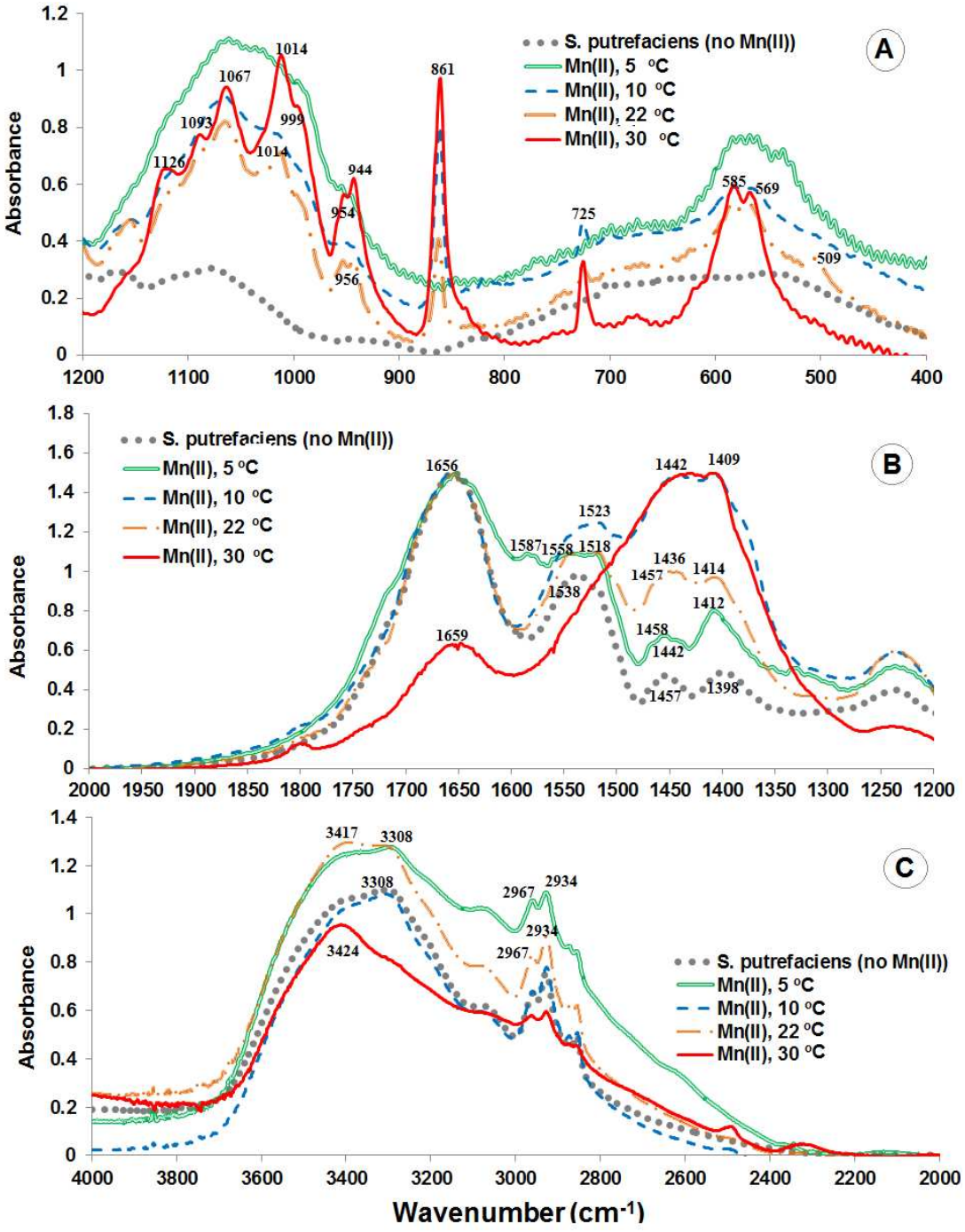


**Fig. 2** FTIR spectra of *S. putrefaciens* in contact with aqueous $Mn^{2+}$ at 400-1300 $cm^{-1}$ (A), 1300-2000 $cm^{-1}$ (B) and 2000-4000 $cm^{-1}$ (C). Experimental conditions: temperatures = 5, 10, 22 and 30 °C; contact time = 30 days; $Mn^{2+}_{initial}$ =200 mg $L^{-1}$; volume of viable bacterial suspension=1000 ml; and bacteria density=2 $g_{dw}$ $L^{-1}$.

Because of the considerable changes in almost all the spectral regions, the spectra are shown in three parts to distinguish the differences. The spectral region of 1200-400 $cm^{-1}$ (Fig. 1A) reflects the largest changes and shows the formation of the two major precipitates (Mn(II) phosphate and Mn(II) carbonate) and the polysaccharides (EPS) produced by the viable cells. The presence of the latter can be concluded from the changes in the bands near 1060 and 580 $cm^{-1}$.[28,29] More detailed study of this spectral region shows that the biosynthesis of the polymeric carbohydrates decreases as temperature increases and is practically absent at 30ºC (in 30 days). However, this conclusion is estimated because the intensity and the dominance of the IR bands in an overlapping area depend on the ratio and the concentration of the substances with IR-active bands. Fig. 1E demonstrates that the amount of precipitates formed at 5°C was much lower than that at other temperatures (10, 22 and 30 °C). In contrast, a large amount of EPS was formed, as is reflected by the broad and intense bands at approximately 1000-1100 and 550-600 $cm^{-1}$ (Fig. 1A), which indicate the presence of EPS, as demonstrated by our colleagues.[28,29]

Because of the overlapping (very intense) carbohydrates bands (which are wider than the bands of the inorganic phases), the formation of Mn(II) phosphate is virtually absent at 5°C in the FTIR spectra; this absence implies that EXAFS studies are required to confirm the biosynthesis of Mn(II) phosphates at 5°C. However, the generation of Mn(II) phosphate at 10, 22 and 30°C is demonstrated by the similarity of the bands near 1060, 1010, 942 and 580 $cm^{-1}$ in the sample data (Fig. 2A) and in the reference spectrum of this compound (Fig. 1SA, Supplementary information). In contrast, the intensity increase in the bands is not proportional because manganese phosphate was not an individual substance; it was one of the constituents in the mixture (microbial biomass, Mn-phosphate and Mn-carbonate) that formed stepwise over a month. The recently formed manganese phosphate most likely interacted with the other particles and molecules as is reflected by the different ratios of the characteristic bands of manganese phosphate in Fig. 2A. However, these characteristic bands of Mn(II) phosphate were the most distinct (sharp) at 22 and especially 30 °C. They were less prominent at 10 °C

and were almost invisible at 5°C because of the overlapping bands from the polymeric carbohydrates formed, called EPS. The broad diffuse bands at 1000-1100 and 550-600 $cm^{-1}$ in the FTIR spectrum of the 5°C sample are so distinct that it is difficult to doubt that a large amount of polymeric carbohydrates is produced by these species at 5°C .[28,30] In addition, as illustrated by the spectrum of the 30°C sample, the band near 580 $cm^{-1}$ grows relatively quickly. This phenomenon can be explained by promotion of the formation of Mn(II) phosphate. Finally, the IR data in Fig. 2A also show the appearance of sharp bands at 861 and 725 $cm^{-1}$ in the FTIR spectra of the three higher temperature samples. These bands perfectly match with those of the reference spectrum of $MnCO_3$ (Fig. 1SB). The presence of this compound is additionally confirmed by the large intensity increase in the band near 1433 $cm^{-1}$ (1409, 1442 $cm^{-1}$) in Fig. 2B. Hence, it is concluded that $MnCO_3$ formed at higher temperatures (10, 22 and 30 °C) but not at 5 °C. The intensity of the characteristic bands of $MnCO_3$ (861, 725, near 1433 $cm^{-1}$) was much lower at 10°C; this difference demonstrates that the least $MnCO_3$ formed at this temperature. Further analysis of the spectral region from 2000-1200 $cm^{-1}$ (Fig. 2B) reveals considerable changes in the region from 1600-1500 $cm^{-1}$, where the amide-II bands are found.[30] The spectrum of the 5°C sample, for instance, shows a small band near 1587 $cm^{-1}$, which is absent in the other samples. This band is additional important evidence of the formation of large amounts of EPS.[28] Additionally, the amide-II band near 1533 $cm^{-1}$ changes shape and position at higher temperatures. We assume that the observed differences are caused by conformational changes in the peptide chain. Shifts in the bands assigned to the carboxylic stretching modes (1398 and 1457 $cm^{-1}$ in the spectrum of *S. putrefaciens* not in contact with $Mn^{2+}$) were only observed for the 5 °C sample. These shifts are evidence that metal complexation to these functional groups was the primary mechanism of $Mn^{2+}$ sorption at the lowest temperature, in contrast to the experiments at 22 and 30 °C in which manganese (II) removal took place through ion exchange (on $H^+$), as reflected by the pH drift in Fig. 1B, D, and F. The band at 1398 $cm^{-1}$ shifted to 1412 and 1414 $cm^{-1}$, the band at 1457 $cm^{-1}$

broadened, and additional bands appeared at 1442 and 1436 $cm^{-1}$ in the samples exposed to Mn(II) at 5 and 10°C. The largest changes in the spectral region from 4000-2000 $cm^{-1}$ (Fig. 2C) are the decrease in the intensity of the amide N-H stretching band (3100-3500 $cm^{-1}$) at higher temperatures and the decreased intensity of the C-H stretching bands near 2934 $cm^{-1}$ of the C-H and OH bends, e.g., polymeric sugars. In our opinion, both phenomena are additional evidence that the formation of polysaccharides is suppressed at higher temperature. The spectra of *S. putrefaciens* (without contact with $Mn^{2+}$) and the sample from the 10°C sorption experiments were practically the same in this region, and in our opinion, this similarity confirms that 10°C is the most comfortable temperature for these microbes. The latest finding is not novel and is in the agreement with the well-known thriving of these species at low temperatures.[31]

**XANES**

Fig. 3 shows the XANES (Mn K-edge) of *S. putrefaciens* exposed to 200 mg $L^{-1}$ of $Mn^{2+}$ at 5, 10, 22 °C over 30 days, at 30 °C – over 10 days, and 5 references: $Mn_3(PO_4)_2$, $MnCO_3$, MnO, MnOOH and $MnO_2$. XANES examination showed that the manganese was divalent in all samples. (No EXAFS spectrum was collected at 30 days for the 30°C sample. The sample was lost.) The inflection point of the absorption edge in the three *S. putrefaciens* samples is at approximately 6542 eV and is evidence of Mn(II) species.[32] For comparison, the (experimental) XANES spectra of trivalent and tetravalent Mn in the reference substances MnOOH and $MnO_2$, respectively, are shown in Fig. 3. The inflection point of the absorption edge in these reference samples are at approximately 6545 and 6547 eV, respectively. The shape of the XANES spectra indicates that the Mn-containing bioprecipitates formed at the interface of the *S. putrefactions* cells are not hydrous oxides. It is obvious that manganese phosphate and manganese carbonates are the two major precipitates. $Mn_3(PO_4)_2$ might be the only precipitate in the 5 °C sample whereas $MnCO_3$ is the dominant precipitate in the 10, 22 and 30 °C samples. The ΔE

values for the all experimental samples shown in Fig. 3 were calculated to be 8.1 eV, Fig. 3. For the references, this value was found to be 8.3, 8.8, 10.1, 8.6, and 17.7 eV respectively for $Mn_3(PO_4)_2$, $MnCO_3$, MnO, MnOOH and $MnO_2$. ΔE value for the two 30 °C samples at 6 and 10 days were calculated to be 8.3 eV.

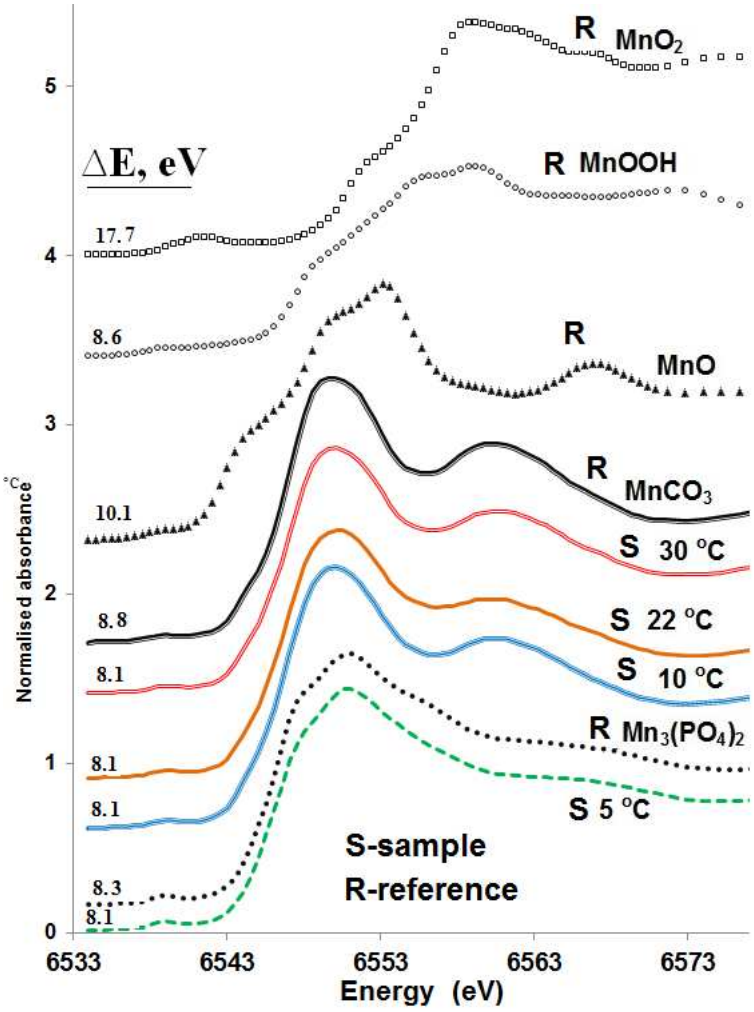


**Fig. 3** XANES of Mn-containing samples of *S. putrefaciens* exposed to 200 mg $L^{-1}$ of $Mn^{2+}$ at 5, 10, and 22 °C over 30 days, and at 30 °C over 10 days and of the references: $Mn_3(PO_4)_2$, $MnCO_3$, MnO, MnOOH and $MnO_2$.

**EXAFS of the samples at 30 days: 5, 10 and 22 °C**

The results from examination of the Mn K-edge EXAFS spectra for the three 30-day samples (5, 10 and 22 °C) are shown in Fig. 4 (A-C) as the XANES linear combination fit. Supplementary information shows the $k^2$- and $k^3$–weighted EXAFS spectra and their Fourier Transforms, Fig. 2S-4S.

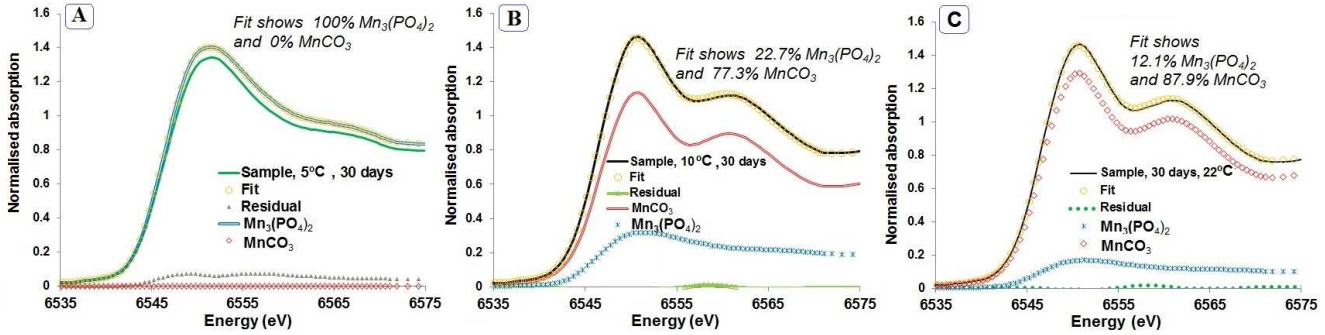


**Fig. 4** The XANES linear combination fits of the *S. putrefaciens* samples exposed to $Mn^{2+}$ for 30 days (contact time) at 5 (A), 10 (B) and 22 (C) °C and of the two references ($MnCO_3$ and $Mn_3(PO_4)_2$). Experimental conditions: microbial density = 2 $g_{dw}$ $L^{-1}$, $Mn_{initial}$ = 200 mg $L^{-1}$, and volume of viable bacterial suspension = 1000 ml.

EXAFS of the 5 °C sample (Fig. 2S) did not show the presence of $MnCO_3$. Linear combination fitting by the Athena program (Fig. 4A) showed that the only precipitate formed at this temperature was $Mn_3(PO_4)_2$. Using any other reference from the list in the experimental section (hydrous oxides and manganese sulphate and chloride) did not change the result of this LCF modelling. Perfect fitting results were achieved for the 10 °C sample, Fig. 4B. These results confirmed the formation of both precipitates, $Mn_3(PO_4)_2$ and $MnCO_3$, and the predominance of $MnCO_3$ (77.3%). The prevalence of $MnCO_3$ in the composition of the precipitates is also obvious from the plots of the $k^2$–weighted EXAFS and the radial structure around the Mn atom (Fig. 3S) of the 10 °C sample with the two references: $Mn_3(PO_4)_2$ and $MnCO_3$. Using EXAFS spectra only, it would be difficult to conclude the presence of manganese phosphate in the 22±2 °C sample (as shown by both the k-weighted EXAFS (Fig. 4S) and the radial structure around the Mn atom (Fig. 4S).

This experimental result is an example of the necessity of applying several spectroscopic techniques to complex environmental samples comprising few various phases. The FTIR spectra reflect the bands of manganese phosphate so distinctly (Fig. 2) that it is difficult to doubt the presence of manganese phosphate in the precipitates, Fig. 2. In addition, the Athena program (which is nicely prepared for complex environmental samples with its linear combination fitting option) allowed perfect LCF result to be achieved and concluded that manganese phosphate composes approximately 12.1% of the Mn-containing precipitates formed at ambient temperature in addition to the primary component (87.9%), manganese carbonate (Fig. 4C).

**EXAFS of the samples with shorter contact times: time dependence of the formation of the major precipitates**

The EXAFS spectra of the few samples collected at less than 30 days were also recorded to observe the temporary changes in the chemical composition of the precipitates formed at 22 and 30 °C. Their linear combination fits are shown in Fig. 5 and 6. Corresponding $k^2$- and $k^3$–weighted Mn K-edge EXAFS spectra and their FTs are shown Fig. 5S-7S. $MnCO_3$ was found to already be the major precipitate (> 50%) at 9 days for an initial $Mn^{2+}$ concentration of 200 mg $L^{-1}$ and at ambient temperature (Fig. 5). The predominance of $MnCO_3$ is also obvious from the comparison of the spectra of *S. putrefaciens* in contact with Mn(II) to those of the references (Fig. 5S and 7S). The percentages of $MnCO_3$ and $Mn_3(PO_4)_2$ precipitated by *S. putrefaciens* on the 9$^{th}$ day as computed by the Athena linear combination fitting model were 64.1 and 33.9 %, respectively, Fig. 5. The fitting result was perfect.

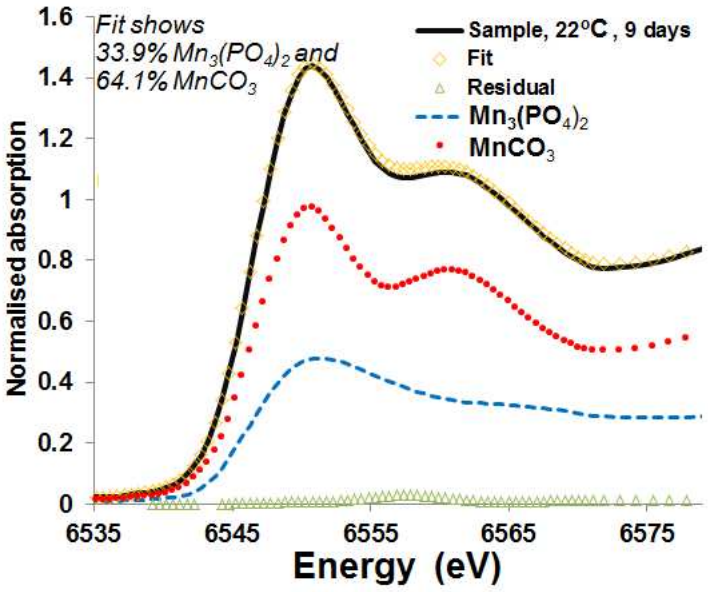


359

360 **Fig. 5** The XANES linear combination fit of the *S. putrefaciens* samples exposed to $Mn^{2+}$ for 9 days at
361 22±2 °C and of the two references ($MnCO_3$ and $Mn_3(PO_4)_2$). Experimental conditions: volume of
362 viable bacteria= 1000 ml; bacteria density=2 $g_{dw}$ $L^{-1}$; and initial $Mn^{2+}$ concentration= 200 mg $L^{-1}$.

363

364 Fig. 6 shows the linear combination fitting results for the *S. putrefaciens* samples exposed to
365 $Mn^{2+}$ for 6 (A) and 10 (B) days at 30 °C. We can conclude from Figs. 6S and 7S that $Mn_3(PO_4)_2$ was
366 the major, or possibly the only, precipitate formed by *S. putrefaciens* for exactly 6 days, even at 30 °C.
367 The Athena LCF stated that the percentage of $Mn_3(PO_4)_2$ was still 96.6% (Fig. 6A). The relative
368 content of $MnCO_3$ found by the program's fitting option was 3.4%; however, without any additional
369 spectroscopic data for this sample (such as FTIR) we prefer to limit our conclusions to the statement
370 that the bioprecipitation of $MnCO_3$ begins in 6 days (to avoid giving the exact percentage of this
371 precipitate in the composition). Continuation of the experiment for 4 more days resulted in a
372 completely different ratio of the two major precipitates in the 10 day sample. The percentages of the
373 main two precipitates in the *S. putrefaciens* sample exposed to Mn(II) over 10 days at 30 °C were
374 computed (Athena LCF) to be 29.1 % for $Mn_3(PO_4)_2$ and 70.9 % for $MnCO_3$, Fig. 6B. Interestingly,
375 these data correlate well with the data for the kinetics of the long-term sorption of Mn(II) (Fig. 1E),

which show a plateau in $Mn^{2+}$ sorption from 2 to 6 days followed by a sharp decrease in the Mn(II) concentration in the solution on the 7th day. It is easy to conclude that this sharp change in the kinetics curve was caused by the formation of the second precipitate, $MnCO_3$.

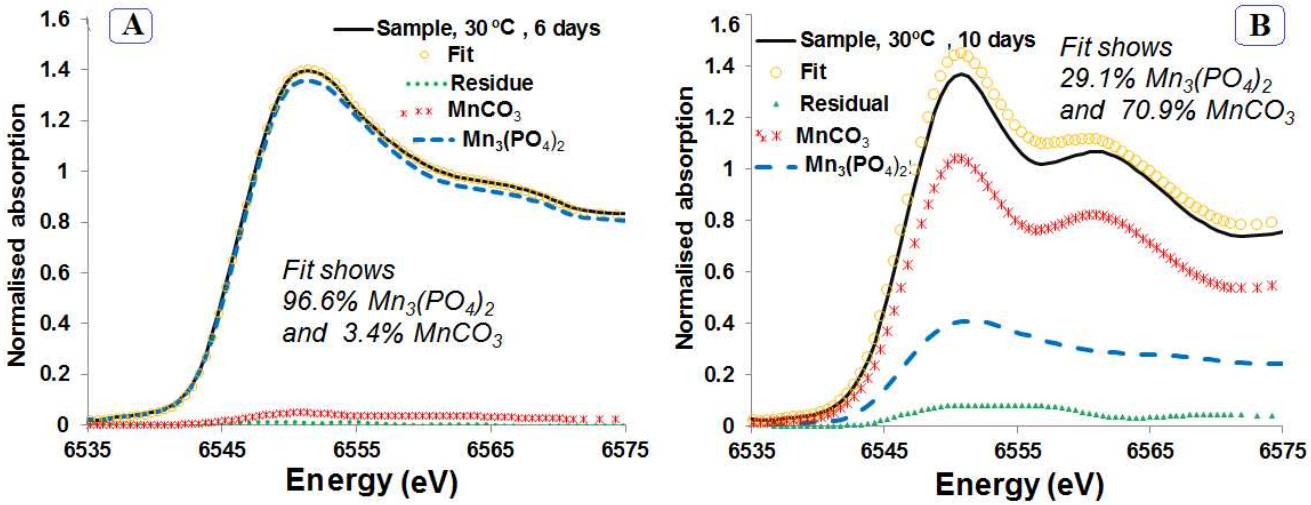


**Fig. 6** The XANES linear combination fits of the *S. putrefaciens* samples exposed to $Mn^{2+}$ for 6 (A) and 10 (B) days of contact time at 30 °C and of the two references ($MnCO_3$ and $Mn_3(PO_4)_2$. Experimental conditions: volume of viable bacteria= 1000 ml; bacteria density=2 $g_{dw}$ $L^{-1}$; and $Mn^{2+}$ initial concentration= 200 mg $L^{-1}$

The rate of generation of $MnCO_3$ was much faster at the highest temperature (30 °C) than at the other temperatures investigated and followed a regular trend: the higher the temperature, the faster the rate of $MnCO_3$ formation, Fig. 1E.

Fig. 7 summarises the data for the ratio of the major Mn-containing precipitates formed at the interface with viable *S. putrefaciens* over 30 days at various temperatures (A) and the (available) data for the percentages of the precipitates at higher (22±2 and 30 °C) temperatures and at various contact times. The data at (22±2 and 30 °C) temperatures are plotted together because of the similarities of the interfacial processes at these temperatures reflected by pH drifts (Fig. 1BDF).

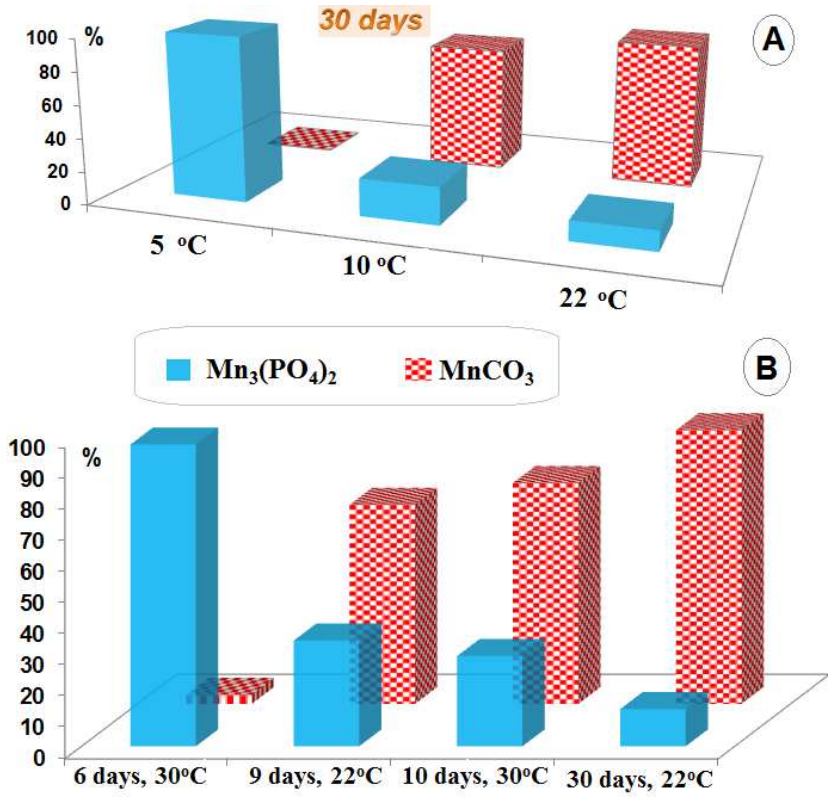


**Fig. 7** Ratio of the main Mn-containing precipitates from IFFEFIT Linear Combination Fitting for the samples at 30 days (A) and temporal dependence of the percentages of the major Mn-containing precipitates from the IFFEFIT Linear Combination Fitting at 22±2 and 30 °C (B). Experimental conditions: $Mn(II)_{initial}$=200 mg $L^{-1}$, microbial density = 2 $g_{dw}$ $L^{-1}$, and batch volume = 1000 ml.

The proportion of manganese carbonate in the composition increased as the temperature increased: from zero at 5 °C to 87.9% at 22±2 °C. At the lowest temperature (5 °C) $Mn_3(PO_4)_2$ was the only precipitate formed by the microbial species investigated. We can conclude (from Fig. 6A) that there is not clear evidence of the presence of $MnCO_3$ in the composition of the bioprecipitates (0-3%) on the $6^{th}$ day; however, on the $9^{th}$ - $10^{th}$ days the percentage of $MnCO_3$ was already 64-70% and showed no distinct temperature dependence over this temperature range (22-30 °C), Fig. 5 and Fig. 6B. After 30 days, the percentage of $MnCO_3$ already reached approximately 88%, Fig. 4C.

406 ## Discussion

407

408 **Different mechanism initiating $Mn^{2+}$ sorption by viable S. putrefaciens at 5-10 °C and 22-30 °C**

409 The long-term sorption (over 30 days) of $Mn^{2+}$ by the viable gram-negative (Mn(IV), Fe(III)
410 reducing) bacterium *S. putrefaciens* is a complex process that includes a few major stepwise reactions.
411 The interfacial processes begins with ion exchange of $H^+$ at 22 and 30 °C, which is reflected in the pH
412 decrease (Fig 1B, D and E); however, a pH decrease was not observed at 5 and 10 °C. Possibly, ion
413 exchange occurs with $Na^+/K^+$ because of a pH increase at 5 and 10 °C; however, ion exchange is not
414 the dominant process. The difference in adsorption mechanisms at various temperatures (higher, 22 and
415 30 °C, and lower, 5 and 10 °C) reflected in the pH change demonstrates the strong influence of
416 microbial viability on the interfacial processes. We think that this factor is a function of two variables:
417 concrete microbial species and the affinity of these species to definite aqueous metal cations. The
418 results of similar experiments might not be the same for every microbial species and every metal
419 cation.

420 We suppose that surface complexation to the functional groups at the bacteria's surface (with no
421 involvement/release of $H^+$) is the main process occurring in the first few days at the lower temperatures
422 (5, 10 °C). Moreover, the FTIR spectrum of the 5 °C sample shows shifts in the bands assigned to the
423 carboxylic groups (evidence of complexation to these groups) that were not observed at ambient
424 temperatures, Fig. 2B.

425

426 **Beginning of Mn(II)-bioprecipitation: rate of Mn(II)-phosphate formation as a function of**
427 **temperature**

428 The bioprecipitation of Mn(II)-containing inorganic phases at the bacterial surface is the continuation
429 of the interfacial reactions that begin 3-4 days after the $Mn^{2+}$ comes into contact with the suspension of

*S. putrefaciens*. The process of bioprecipitation always begins with the formation of Mn(II) phosphate at any of the investigated conditions[24] and larger batches, various concentrations of $Mn^{2+}$ and various temperatures (5, 10, 22 and 30 °C). This substance remains the major component of the precipitate for more than 1 week at any of the mentioned conditions. The formation of $Mn_3(PO_4)_2$ can be explained by the release of intracellular inorganic phosphorus and/or protein-like substances (containing phosphate groups) into solutions of the still viable bacteria. Schematic interaction of $Mn^{2+}$ and $PO_4^{3-}$ mediated by viable *S. putrefaciens* can be shown: $Mn^{2+} + PO_4^{3-} \xrightarrow{viable\ cells} Mn_3(PO_4)_2\downarrow$

The ability of many microbial species to accumulate inorganic phosphorus intracellularly and to release it under suitable circumstances is a well-known phenomenon.[33-37] Van Veen[37] demonstrated that phosphate uptake through the phosphate inorganic transport system (Pit) is dependent on the presence of divalent cations (such as $Mg^{2+}$, $Ca^{2+}$, $Co^{2+}$, $Mn^{2+}$), which form a soluble, neutral metal phosphate ($MeHPO_4$); however; the trend for Mn(II)-dependence was not reported. Many Luria Bertani precursors are prepared with a phosphate buffer. Viable cells of *S. putrefaciens* seemed to accumulate phosphate intracellularly while they grew in the Luria Bertani solution for two days. They started to release the phosphate within a few days for their physiological needs. The released phosphorus (at lower concentrations) was employed by the same species for the surface precipitation of Mn(II) phosphate. Phosphorus concentration measured in parallel experiments was never higher than 200 mg/L as shown in the previous work[24]. It ranged 20-120 mg/L. Within approximately one week, the viability of the living bacteria was depressed (as was demonstrated by few microbiological plate experiments), and the release of phosphate-containing protein-like substances was also decreased. It is possible that the release of the intracellular inorganic phosphorus stopped because of the partial inactivation of viable cells. The absence of inorganic phosphorus release made the formation of Mn(II) phosphate impossible, as was reflected in the absence of Mn(II) removal for a few days, within 2-5 days for the most investigated temperatures (Fig. 1E). However, the partial inactivation of *S.*

*putrefaciens* cells created different physicochemical conditions in the experimental suspensions that allowed $MnCO_3$ to be formed.

**Later stage precipitation: $MnCO_3$ (≥ 1 month contact time) only in larger batches and only at higher temperatures ( ≥ 10 °C)**

$MnCO_3$ formed in the larger (1000 ml) batches only (in which *S. putrefaciens* was viable for a much longer time than in the smaller (125 ml) batches, as shown in Chubar et al. 2013) but only at temperatures ≥ 10 °C. The formation of $MnCO_3$ did not start at the same time as the formation of $Mn_3(PO_4)_2$ but became the dominant process at a later stage. In the first < 6 days, $Mn_3(PO_4)_2$ was still approximately 100 %, even for the 30 °C experiment (Fig. 6A), in which the formation of $MnCO_3$ was the most intense, as was reflected in the fast, sharp decrease of the Mn(II) concentration in the solution (Fig. 1E), and the highest bands of FTIR spectra at 725 and 861 $cm^{-1}$ assigned to $MnCO_3$. During the first <6 days, when the formation of $Mn_3(PO_4)_2$ was the main process (and $MnCO_3$ was absent), *S. putrefaciens* was still 80% viable and capable of reproducing. The $MnCO_3$ process became dominant when (1) most of the bacterial cells no longer appeared viable. The process can be promoted by increasing the pH value (Fig. 1F) and occurs if the concentrations of both $Mn^{2+}$ and carbonate (accumulated through $CO_2$ uptake) become sufficiently high.

Rise in pH resulted in increase of bicarbonate and carbonate anions (through $CO_2$ accumulation from air). These anions became available for the interaction with $Mn^{2+}$ and both ions used by bacterial cells to precipitate $MnCO_3$ in accordance with the schematic reactions:

$$CO_{2(aq)} + H_2O \leftrightarrow H_2CO_3 \quad \text{(at low pH values, ~4)}$$

$$CO_{2(aq)} + OH^- \leftrightarrow HCO_3^- \quad \text{(formation of } HCO_3^- \text{ dominates at pH > 6)}$$

$$HCO_3^- + OH^- \leftrightarrow CO_3^{2-} + H_2O \quad \text{(dominates at > pH 9)}$$

$$Mn^{2+} + CO_3^{2-} \xrightarrow{viable\ cells} MnCO_3\downarrow \quad \text{(precipitated by } \textit{S. putrefacines}\text{)}$$

Until phosphate became available in the solution, the formation of Mn(II) phosphate was the main precipitation process because of the solubility constant of Mn(II) phosphate ($LogK_s$ = - 27.07)[38] compared to $MnCO_3$ ($LogK_s$ = - 10.58).[39] Concentrations of phosphorous in natural waters, pore solutions of soils and bottom sediments is <<1 mg/L.[40] Concentration of Mn(II) in natural waters is <0.05 mg/L.[41] Such concentrations of both Mn(II) and phosphate exclude a possibility of Mn phosphate precipitation based on the mineral solubility (without direct or indirect involvement of viable or non-reproducible microbes). As well as manganese phosphate, $MnCO_3$ could not be formed under the given experimental conditions without microbial activity. In order to synthesise $CaCO_3$ researchers were continuously bubbling $CO_2$ into 0.1 mol/L $CaCl_2$ at pH 9.85.[42] We did not bubble $CO_2$ into our experimental batches and the flasks were closed (covered by the caps) for >90% of the experiment. pH was not higher than 8.3.

**The role of the microbial metabolic activity on the ratio of the main Mn(II)-precipitates at various temperatures (5, 10, 22 and 30°C) and on the formation of EPS**

The processes at the interface of *S. putrefaciens*-$Mn^{2+}$ aqueous at 5 °C were different than those at 10, 22 and 30 °C, and these differences were reflected in the kinetics of the Mn(II) sorption (Fig 1ACE) and were demonstrated by the FTIR and EXAFS investigations. $MnCO_3$ did not form after 30 days at 5 °C (Fig. 2, 4A). $Mn_3(PO_4)_2$ was the only precipitate detected by EXAFS (Fig. 4A). We observed that at 5 °C, *S. putrefaciens* cells were viable for a longer time than at the higher temperatures. We do not present quantitative results for the cells' viability. Several tests were performed. They indicated that at all the investigated temperatures, the microbes were at least 60 % viable for the first 5 days. It was also obvious (visually) that the microbes became inactivate faster at higher temperatures when their natural pink colour became grey. At 5 °C, the pink colour did not change to grey for almost 2 weeks. In contrast, at 30 °C, the colour became greyish after 6 days. This result means that the stronger metabolic

activity of the living cells was an important factor that influenced the processes at the interface. We suppose that if the experiments were continued for longer times, a sharp decrease could be observed for the $Mn^{2+}$ in the solution and the $MnCO_3$ could be detected later (because of the sharp decrease of the Mn(II) concentration), but this hypothesis must be tested.

We must remark here that the formation of ESP was so intense at 5 °C that it was not possible to detect the Mn(II) phosphates by FTIR alone because of the overlapping bands of from the polymeric sugars (which are wider than the bands for phosphate). We can conclude, however, that the freshly formed ESP did not visibly contribute to the continuation of $Mn^{2+}$ removal from the solution, and this result differs from the literature data on the strong removal capacity of EPS.[43-45] However this result is similar to those obtained by the other colleagues who reported that the EPS-bearing systems of *Pseudomodas putida* did not enhance the removal of Cd relative to EPS-free system.[46] It is possible that if we separated the EPS, it could sorb metal ions; however, in the presence of *S. putrefaciens* cells at the higher density of 2 $g_{dw}$ $L^{-1}$, the processes of Mn(II) phosphate and Mn(II) carbonate bioprecipitation were dominating at the conditions described in this work.

## Conclusions

The data shown in this work demonstrate that viable *S. putrefaciens* (and most likely some other microorganisms) has a great potential to stabilise (or reduce the mobility in the environment of) $Mn^{2+}$ (and most likely some other metal ions) through processes occurring at the interfaces of the cells for at least 30 days. After initial contact with $Mn^{2+}$, the interfacial processes resulted from the bacteria surface chemistry and the role of ion exchange (of $H^+$) or complexation (with no involvement/release of $H^+$) depended on the temperature. Several days after the viable cells of *S. putrefaciens* came into contact with the $Mn^{2+}$, they precipitated a Mn-containing inorganic phase. The chemical composition of the new inorganic phase was greatly dependent on the metabolic activity of the viable microbes, which

529 was, first of all, a function of the temperature, the total amount of cells and the metal loading.
530 Temporary changes in the composition of the new inorganic phase may also depend on the solubility
531 constants of the inorganic precipitates and the availability of the corresponding anions in the solution.

532 Ion exchange of $H^+$ was the main process that initiated the processes at the interface of *S.*
533 *putrefaciens*-$Mn^{2+}$ at 22 and 30 °C; however, at 5 and 10 °C, (probably) because of much stronger
534 hydrogen bonding, metal complexation with the microbial surface functional groups (at least,
535 carboxylic groups) was the initial step. In the 1000-ml batches with a bacteria density of 2 $g_{dw}$ $L^{-1}$, the
536 two major Mn-containing inorganic phases ($Mn_3(PO_4)_2$ and $MnCO_3$) formed at 10, 22 and 30 °C, but
537 only one main phase ($Mn_3(PO_4)_2$) was detected at 5 °C over 30 days. The formation of $MnCO_3$ started
538 later (after 6 days) when the viable cells no longer provided intracellular inorganic phosphorus and
539 when the pH of the solution became higher.

540 In the presence of *S. putrefaciens* cells, Extracellular Polymeric Substances (EPS) did not
541 contribute to the $Mn^{2+}$ removal; however, they might sorb manganese(II) ions when preliminarily
542 separated from the bacterial biomass.

543

544

545 ## Acknowledgements

546

547 Financial support under the form of the European Union Marie Curie IIF Fellowship to N. Chubar
548 (grant № MIF1-CT-2006-021922) and Dutch Ministry of Scientific Research NWO (grant №
549 195.068.281) funded the EXAFS/XANES studies at BM26A of ESRF (experiment № 26-01-794) are
550 gratefully acknowledged. We thank the anonymous reviewers and the editor who helped to improve
551 this work considerably.

552

553 **Supplementary information**

554 Supplementary data associated with this work can be found online:

555

556 ## References

557


558 1. F.G. Ferris, T.J. Beveridge, W.S. Fyfe, *Nature* 1986, **320**, 609-611.

559 2. F.G. Ferris, W.S. Fyfe, T.J. Beveridge, Chem. Geol. 1987, **63**, 225-232.

560 3. F.G. Ferris, C.M. Fratton, J.P. Gerits, S. Schultze-Lam, B. Sherwood Lollar, Geomicrobiol. J., 1995,
561 **13**, 57-67.

562 4. A.H. Reidies, Manganese Compounds: Ullmann's Encyclopedia of Chemical Technology, John
563 Wiley. 2007.

564 **5.** Y. Tang, S.M. Webb, E.R. Estes, C. M. Hansel, *Environ. Sci.: Processes Impacts***,** 2014, **16,** 2127-
565 2136.

566 6. D.L. Lovley, (Ed.) Environmental-microbe metal interaction. ASC press. Washington DC. 2000.

567 7. J.J. Morgan, Manganese in Natural Waters and Earth's Crust. Its Availability to Organisms, in
568 Manganese and Its Role in Biological Processes: Metal Ions in Biological Systems A Sigel and H.
569 Sigel Eds Dekker M, New York. 2000, **27**, 1-34.

570 8. J.J. Morgan, *Geochim. et Cosmochim. Acta,* 2005, **69**, 35-48.

571 9. B.M. Tebo, J.R. Bargar, B.G. Clement, G.J. Dick, K.J. Murray, D. Parker, R. Verity, S.M. Webb,
572 *The Annual Review of Earth and Planetary Sciences* 2004, **32**, 287-328.

573 10. D.J. MacDonald, A.J. Findlay, S.M. McAllister, J.M. Barnett, P. Hredzak-Showalter, S.T. Krepski,
574 S.G. Cone, J. Scott, S.K. Bennett, C.S. Chan, D. Emerson, G.W. Luther III, *Environ. Sci.:*
575 *Processes Impacts*, 2014, **16**, 2117-2126.

576 11. Y.M. Nelson, L.W. Lion, W.C. Ghiorse, M.L. Shuler, Appl. Environ. Microbiol., 1999, **65**, 175–
577 180.
578 12. K. Tazaki, *Clays and Clay Minerals* 1997, **45**, 203-212.
579 13. S.M. Webb, B.M. Tebo, J.R. Bargar, *American Mineral.,* 2005, **90**, 1342-1357.
580 14. K. Nealson, The Manganese-Oxidizing Bacteria (chapter 3.1.10) in: Prokaryotes. Springer New
581 York 2006, 222-231.
582 15. A.S. Templeton, H. Staudigel, B.M. Tebo, *Geomicrobiol. J.*, 2005, **22**, 127–139.
583 16. J. Mukhopadhyay, J. Gutzmer, N.J. Beukes*, J. Earth System Scie.,* 2005, **114**, 247-257.
584 17. D. Fan, J. Ye, L. Yin, R. Zhang, *Ore Geology Reviews* 1999, **15**, 79-93.
585 18. A.R. Kampf, P.B. Moore, *American Mineralogist* 1976, **61**, 1241-1248.
586 19. A-M. Fransolet, M.A. Cooper, P. Cerny, F.C. Hawthorne, R. Chapman, J.D. Grice, *The Canadian*
587 *Mineralogist,* 2000, **38**, 893 – 898.
588 20. M.A. Cooper, F.C. Hawthorne, P. Cerny, *The Canadian Mineralogist* 2009, **47**, 173 – 180.
589 21. M. Polgári, M.S. Drubina, Z. Szabó, *Bulletin of Geosciences,* 2004, **79**, 53–61.
590 22. P.M. Okitar, W.C. Shanks*, Chemical Geol.,* 1992, **99**, 139-164.
591 23. D.A. Bazylinski, R.B. Frankel, *Reviews in Mineralogy and Geochemistry* 2003, **54**, 217-247.
592 24. N. Chubar, T. Visser, C. Avramut, H. De Waard, *Geochim. et Cosmochim. Acta,* 2013, **100**, 232-
593 250.
594 25. R.J. Haas, Chem. Geol., 2004, **209**, 67–81.
595 26. S. Nikitenko, A. Beale, A. van der Eerden, S. Jacques, U. Leynaud, M. Óbrien, D. Detollenaere, R.
596 Kaptein, B. Weckhuysen, W. Bras, *J. Synchrotron Radiation*, 2008, **15**, 632-640.

27. B. Ravel, M. Nevwille, *J. Synchrotron Radiation*, 2005, **12**, 537-541.

28. F. François, C. Lombard, J.M. Guigner, P. Soreau, F. Brian-Jaisson, G. Martino, M. Vandervennet, D. Garcia, A.L. Molinier, D. Pignol, J. Peduzzi, S. Zirah, S. Rebuffat, *Appl. Environ. Microbiol.,* 2012, **78**, 1097-106.

29. R. Mikutta, U. Zang, J. Chorover, L. Haumaier, K. Kalbitz, *Geochim. et Cosmochim. Acta,* 2011, **75**, 3135-3154.

30. G. Socrates, Infrared Characteristic Group Frequencies, John Wiley & Sons New York. 1994.

31. H.H. Hau, J.A. Gralnick, *Annual Reviews in Microbiol.,* 2007, **61**, 237–58.

32. B.L. Stueben, B. Cantrelle, J. Sneddon, J.N. Beck, *Microchem. J.,* 2004, **76**, 113–120.

33. T. Berman, G.W. Skyringt, Phosphorus cycling in aquatic microorganisms studied by phased uptake of $^{33}P$ and $^{32}P$. Current Microbiology 1979, **2**, 47-49

34. H. Ohtake, K. Takahashi, K. Toda, *Wat. Res.,* 1985, 1587-1594.

35. R.E. Blake, J.R. O'Neil, G.A. Garcia, *American Mineral.,* 1998, **83**, 1516-1531.

36. B.L. Turnet, J.P. Driessen, P.M. Haygarth, I.D. Mckelvie, *Soil Biol. Biochem,,* 2003, **35**, 187-189.

37. H.W. Van Veen, T. Abee, G.J.J. Kortstee, W.N. Konings, A.J.B. Zehnder, Biochem., 1994, **33**, 1766-1770.

38. G. Friedl, B. Wehrli, A. Manceau, A., Geochim. et Cosmochim. Acta, 1997, **62**, 275-290.

39. K.S. Johnson, Geochim. et Cosmochim. Acta, 1982, **46**, 1805-1809.

40. A.O. Fadiran, S.C. Dlamini, A. Mavuso, Bull. Chem. Soc. Ethiop., **2008**, 22, 197-206

41. http://www.hc-sc.gc.ca/ewh-semt/pubs/water-eau/manganese/index-eng.php

42. H. Watanabe, Y. Mizuno, T. Endo, X. Wang, M. Fuji, M. Takahashi, Advanced Powder Technology, 2009, **20**, 89-93.

43. L. Fang, S. Yang, Q. Huang, A. Xue, P. Cai, *Chem. Geol*. 2014, **386**, 143-151.

44. J. Tourney, B.T. Ngwenya, J.F.W. Mosselmans, M. Magennis, J. Coll. Interf. Scie., 2009, **337,** 381-389.

45. S.P. de Oliveira Martins, F.N. de Almeida, S. Gomes Ferreira Leite, *Brazilian J. Microbiol.,* 2008, **39**, 780-786.

46. M. Ueshima, B.R. Ginn, E.A. Haack, J.E.S. Szymanowski, J.B. Fein, Geochim. et Cosmochim. Acta, 2008, **72**, 5885-5895.